Deeply inelastic scattering of ^{84}Kr from ^{208}Pb†

R. Vandenbosch and M. P. Webb
University of Washington, Seattle, Washington, 98195

T. D. Thomas
Oregon State University, Corvallis, Oregon 97331

(Received 2 September 1975; revised manuscript received 5 April 1976)

We report here energy spectra and angular distributions for deeply inelastic scattering of ^{84}Kr from ^{208}Pb at laboratory energies of 494, 510, and 718 MeV. The deeply inelastic process is found to be the dominant reaction process at all energies investigated. At the highest bombarding energy the most probable kinetic energy of the deeply inelastic component becomes progressively larger as the grazing angle is approached, in contrast to near barrier energies where the most probable kinetic energy remains more nearly independent of angle. A semiclassical calculation of the deeply inelastic angular distributions, employing the deflection functions calculated from an optical model potential that reproduced the elastic scattering in this system, is shown to reproduce the deeply inelastic scattering at the lower energies.

[NUCLEAR REACTIONS ^{208}Pb(^{84}Kr, X), E = 494, 510, and 718 MeV; measured energy spectra and $\sigma(\theta)$ for quasielastic and deeply inelastic reaction products. Obtained integrated σ; compared with optical model absorption σ: Deflection function analysis.]

I. INTRODUCTION

The study of reactions between heavy projectiles and heavy targets has led to the observation[1-6] of a new kind of reaction process which dominates the total reaction cross section. This process, variously referred to as deeply inelastic scattering, quasifission, or strongly damped collisions, is characterized by reaction products with masses close to those of the projectile and target, angular distributions peaked near the grazing angle, and kinetic energy distributions corresponding to large energy losses. One of the most remarkable features of these reactions is the ability of the nuclear system to convert hundreds of MeV of relative kinetic energy into internal excitation and deformation energy on the short time scale implied by the angular distributions and with little redistribution of nucleons between the projectile and target.

Early studies of this process with Kr or comparable mass projectiles were performed at energies close to the Coulomb barrier where the Coulomb deflection dominates the trajectories and most partial waves have classical trajectories that do not result in very intimate contact of the projectile and target. In this paper we report energy spectra and angular distributions for deeply inelastic scattering of ^{84}Kr nuclei by ^{208}Pb at laboratory energies of 494, 510, and 718 MeV. This study extends to bombarding energies well above the Coulomb barrier where the distance of closest approach becomes small enough that one might expect considerable amalgamation on the basis of previously suggested criteria.[7] Instead we find angular distributions and integrated cross sections which indicate that deeply inelastic scattering is the dominant reaction even at the highest bombarding energy studied. These results have been summarized in a recent letter.[6] In the present paper we describe these results in greater detail and also report on the kinetic energy distributions and their dependence on angle and bombarding energy. The angular distributions are interpreted in terms of deflection functions calculated from optical model potentials.

II. EXPERIMENTAL PROCEDURE

Krypton beams from the Lawrence Berkeley Laboratory SuperHILAC (heavy-ion linear accelerator) were used to bombard a 50-μg/cm^2 target of ^{208}Pb (99.14% isotopically pure). The beam was collimated to 0.32 cm diameter at the target. Typical beam currents were about 1–2 particle nA.

Singles spectra were obtained with two heavy-ion surface-barrier detectors. Each subtended a solid angle of 1.4 msr at the target and had an acceptance angle of 0.75° (lab) in the reaction plane. A third detector was placed at a fixed laboratory angle of 30° to monitor the beam energy and structure and the target thickness. Signals from these detectors were amplified with conventional electronics, digitized by an analog multiplexer coupled to a single analog-to-digital converter, and presented to a PDP-15 computer. The computer

stored the data for subsequent analysis and provided an on-line display of the three spectra as data were collected. The dead time was checked using a pulser triggered by a monitor counter. Corrections did not exceed 25%.

The elastic peak typically had a full width at half maximum of 8–10 MeV. A kinematic spread of 2.4 MeV was expected from the finite angular acceptance of the detectors. The spread due to energy loss in the target was approximately 0.6 MeV. The remaining width was due to detector resolution and the energy dispersion of the beam. Occasionally there appeared to be two energy components in the beam, separated by several MeV.

At forward angles large numbers of electrons from the target could produce sizable signals in the detectors. These were suppressed by biasing the target (1 kV), inserting a thin nickel foil (100 $\mu g/cm^2$) between the target and the detectors, and by providing a magnetic field to deflect electrons away from the detectors.

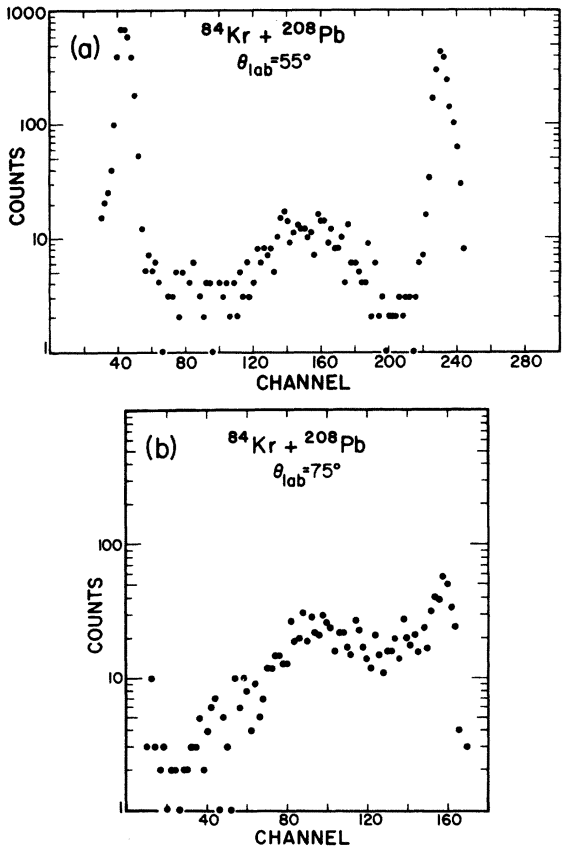

FIG. 1. Energy spectra at 494 MeV for (a) 55° and (b) 75° (lab). The low energy peak in (a) at channel 50 corresponds to recoiling ^{208}Pb nuclei. At 75° the valley between the deeply inelastic and elastic peaks has filled with quasielastic events.

The absolute cross sections were obtained by normalizing the observed elastic counting rate to Rutherford scattering at forward angles.

III. RESULTS

Energy spectra taken at 55° and 75° (lab) with a 494-MeV Kr beam are shown in Fig. 1. At most angles the deeply inelastic events are well separated from the other reaction products [Fig. 1(a)] whereas, near the grazing angle (the angle where $\sigma_{el}/\sigma_R = \frac{1}{4}$) the region between the deeply inelastic

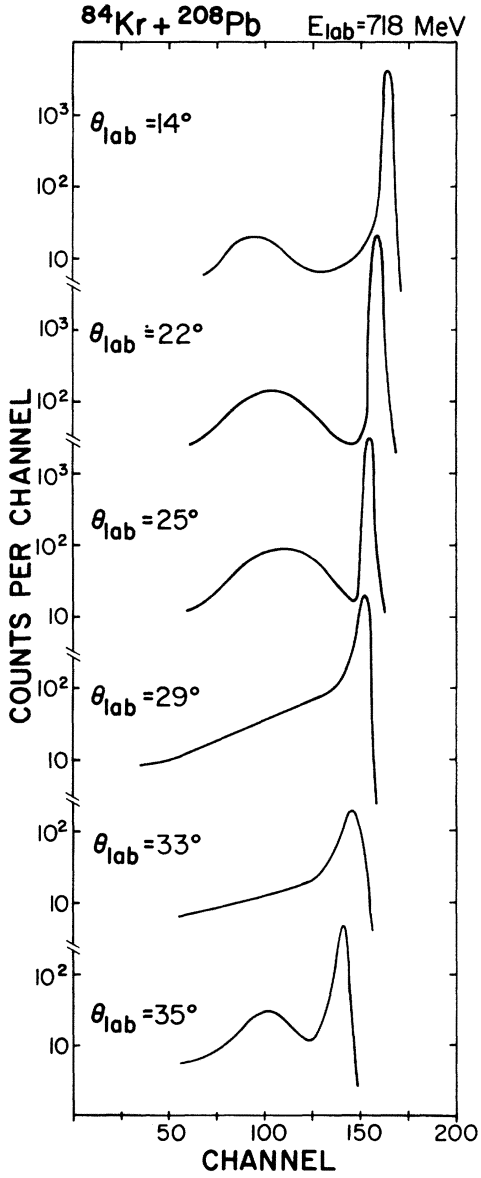

FIG. 2. Energy spectra for 718-MeV $^{84}Kr + ^{208}Pb$. Only the shapes of the energy spectra are shown; the relative cross sections at the different angles are not indicated in this figure.

and elastic peaks fills up with "quasielastic" events [Fig. 1(a)]. The deeply inelastic component at this energy exhibits a most probable kinetic energy consistent with complete damping of the incident kinetic energy, nearly independent of angle. At 718 MeV the kinetic energy spectra show a pronounced difference. Figure 2 displays the energy spectra at different angles for this higher energy. As is evident from the figure, the deeply inelastic peak moves up in energy as the grazing angle is approached until very near the grazing angle [~35° (lab) at this energy] the valley between the deeply inelastic component and the elastic peak is filled with quasielastic events. These quasielastic processes are inelastic and transfer reactions in which the energy loss is more typical of that encountered for direct reactions with lighter projectiles.

A more complete overview of the relative energy dependences of these various processes may be obtained from a contour map of $d^2\sigma/dE_{c.m.}d\Omega$ as shown in Fig. 3 where $E_{c.m.}$ is the exit channel total kinetic energy. This energy was calculated from the observed light-particle kinetic energy assuming two-body kinematics with the observed and unobserved particles having the masses of the projectile and target, respectively. As can be seen, the deeply inelastic peak is well defined at angles less than the grazing angle, merges with the quasielastic events near the grazing angle and becomes well separated again at angles larger than the grazing angle. The most probable exit channel total kinetic energy for the deeply inelastic scattering in the 718-MeV experiment is shown as a function of angle in Fig. 4. At this bombarding energy there are sizable corrections that have to be made to the light fragment kinetic energies to obtain the total kinetic energy in the exit channel. First, neutron emission can change the observed kinetic energy from that of the primary particle. Second, the assumption of no mass transfer, i.e., that the light and heavy particles conserving momentum in the exit channel have the masses of the projectile and target, is less likely to be valid at 718-MeV bombarding energy than at 494 MeV. It is nevertheless clear that the energy loss increases for angles both larger and smaller than the angle corresponding to the peak of the angular distribution.

The angular distributions obtained in this work at E_{lab} = 494, 510, and 718 MeV are presented in Fig. 5. The resolution of the energy spectra near the grazing angle into elastic and nonelastic events was achieved by fitting the shape of the elastic peak at a more forward angle than the angle being analyzed, and using this shape to determine the elastic contribution at the angle being considered. It is difficult to decompose further the energy spectra into quasielastic and deeply inelastic

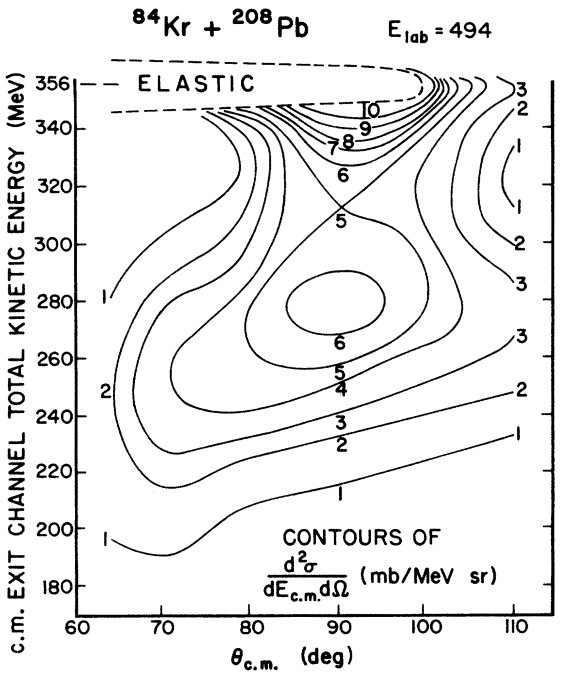

FIG. 3. Contours of $d^2\sigma/dE_{c.m.}d\Omega$ for 494-MeV bombardment of ^{84}Kr + ^{208}Pb.

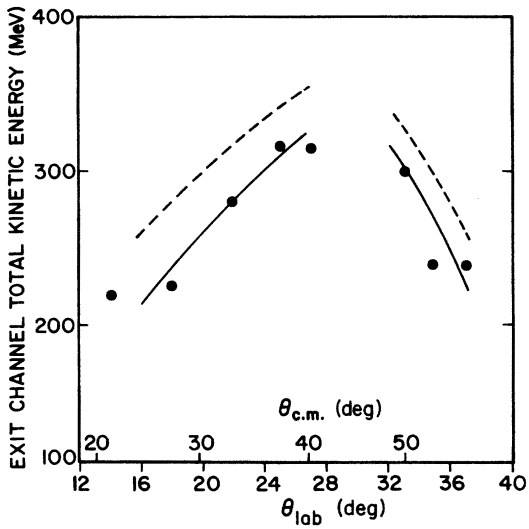

FIG. 4. Exit channel total kinetic energy at 718 MeV as a function of angle. The points and full curve are based on the light-particle energy and the assumption that observed and recoil particles have the same masses as the projectile and target, respectively. The dashed curve is the result after correction for neutron emission assuming that one neutron is emitted for every 10 MeV of inelasticity, that the excitation energy is divided in proportion to the masses, and that there is no mass transfer.

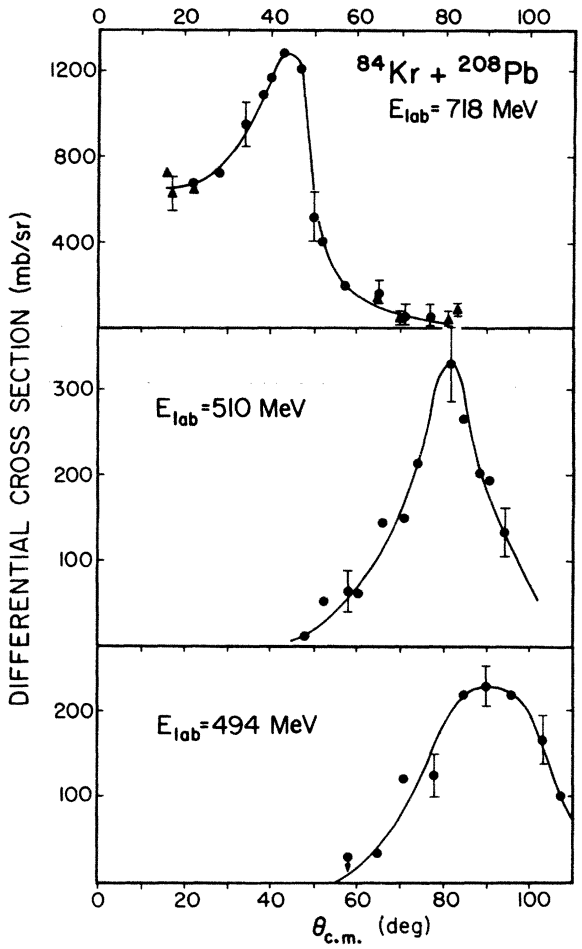

FIG. 5. Deeply inelastic angular distributions for ^{84}Kr and ^{208}Pb.

events. It is not at all apparent that a clear distinction between the two processes is to be expected. The cross sections in Fig. 5 include both these processes. We use the term deeply inelastic scattering in the discussion that follows to include all of the nonelastic cross section. The maximum in the angular distribution is typically slightly forward of the angle at which the elastic cross section has fallen to $\frac{1}{4}$ of that for Rutherford scattering, and moves forward with increasing energy. In addition, the peak in the angular distributions becomes sharper as the energy is increased.

IV. DISCUSSION

The angular distributions presented in Fig. 5 exhibit peaks that both move forward and become increasingly sharper as the bombarding energy is increased. Both of these features can be understood in terms of the influence of the attractive nuclear potential. The deeply inelastic scattering arises from lower partial waves than the elastic scattering and hence is more strongly influenced by the nuclear potential. The sharpening of the peak with increasing energy can be attributed to a focusing effect whereby low partial waves, which experience the greatest Coulomb repulsion and lead to large angle scattering at low energy, at higher energies penetrate sufficiently into the region of the attractive potential to be bent forward toward the same angles as higher partial waves experiencing both less Coulomb and less nuclear deflection. At the lower bombarding energy there is no evidence for orbiting as suggested by Wilczynski[8] in the interpretation of reactions in the $^{40}Ar + ^{232}Th$ system. At the highest energy the slower rate of decrease in the differential cross section at forward angles may be an indication of a contribution from this process. There is very recent evidence[9,10] that for lighter targets orbiting can occur even with Kr projectiles. It also might be expected to become more important at still higher energies in the present system. Tamain *et al.*[11] have recently reported results on the $^{63}Cu + ^{197}Au$ system which indicate that, for the fully damped component only, at 365 MeV orbiting is negligible while at 443 MeV there is evidence for orbiting.

We have attempted to decompose the spectrum of reaction products at 718 MeV in a way similar to that done in Ref. 11 so as to obtain an angular distribution indicative of the behavior of only the fully damped events. In doing so there still remains a pronounced peaking of the angular distribution in contrast to the $^{63}Cu + ^{197}Au$ system at 443 MeV where the cross section $d\sigma/d\Omega$ falls smoothly with angle. The maximum in the angular distribution for the fully damped events occurs approximately 5° lower than that for the angular distribution shown at the top of Fig. 5. It appears that orbiting is very sensitive to the Z_1Z_2 product of the system and to the energy above the barrier. We interpret our 718-MeV data as being consistent with the onset of orbiting but that the largest fraction of the reaction cross section can still be attributed to a relatively fast reaction process peaked near the grazing angle. We expect that the two different angular components do not arise from fundamentally different mechanisms but rather are extensions of the same process.

It is possible to achieve a qualitative understanding of the angular distributions by examination of the deflection functions derived from optical model calculations. A more quantitative account of the angular distributions can be developed from the classical cross section expression and these deflection functions, particularly if the inelasticity and distortion in the exit channel are taken into account. Such a semiclassical approach seems

justified since the wavelength of the relative motion is very small (0.03 fm) compared to the radii of the ions (5–10 fm) and since very large angular momenta ($l \sim 100$–200) are contributing to the reaction. In fact, the criteria for applicability of a semiclassical model are perhaps better met by this system than by any other nuclear system studied to date. The deflection functions for 494- and 600-MeV bombarding energies are shown in Fig. 6. The dashed lines give the deflection due to the Coulomb and centrifugal potentials, while the full curves include also the effects of the nuclear potential. The latter curves have been constructed using the identification for the deflection function[12]

$$\theta(l) = 2\frac{d\delta_l}{dl},$$

where δ_l is the real part of the scattering phase shift. The phase shifts have been calculated from optical model potentials that reproduce the elastic scattering.[13] The effect of the real part of the nuclear potential is to make the deflection angle smaller than that for the Coulomb and centrifugal potential alone for those partial waves with significant amplitudes within the range of the potential. An arrow in the figure indicates the l value for which T_l, the optical model transmission coefficient, becomes $\frac{1}{2}$. Thus, the deflection function for l values to the left of the arrow corresponds primarily to deeply inelastic scattering, whereas those to the right of the arrow correspond to elastic scattering. Two features emerge as the bombarding energy is increased. First of all, the deflection angles for l values less than those for which $T_l = \frac{1}{2}$ decrease, accounting for the forward movement of the peak in the angular distributions with increasing energy. Secondly, the dependence of the deflection angle on l becomes weaker so that more l values are concentrated in a particular angular range as the energy increases. This results in a sharper peaking of the angular distribution. More quantitatively, this effect arises from the $d\theta/dl$ factor in the denominator of the classical cross section expression[12]

$$\left(\frac{d\sigma}{d\Omega}\right)_{cl} = \frac{l}{\sin\theta}\,\frac{1}{k^2(d\theta/dl)},$$

where k is the wave number of the relative motion and θ is the deflection angle.

The deflection function as defined above is sensitive to the imaginary as well as to the real part of the nuclear potential, as has been discussed by Harney, Braun-Munzinger, and Gelbke[14] and by Gelbke.[15] The absorptive part of the potential can introduce an additional deflection of the incident particles. The imaginary potentials determined from the elastic scattering fits are rather weak, so that the effect on the deflection function becomes significant only at the higher bombarding energies. The effect at 600 MeV is illustrated in Fig. 6(b) where the deflection functions with $W = 2.5$ MeV (full curve) and $W = 0.1$ MeV are compared (dashed-dot curve); the effect at 494 MeV is negligible. Since we are applying the deflection function to those processes that are treated as

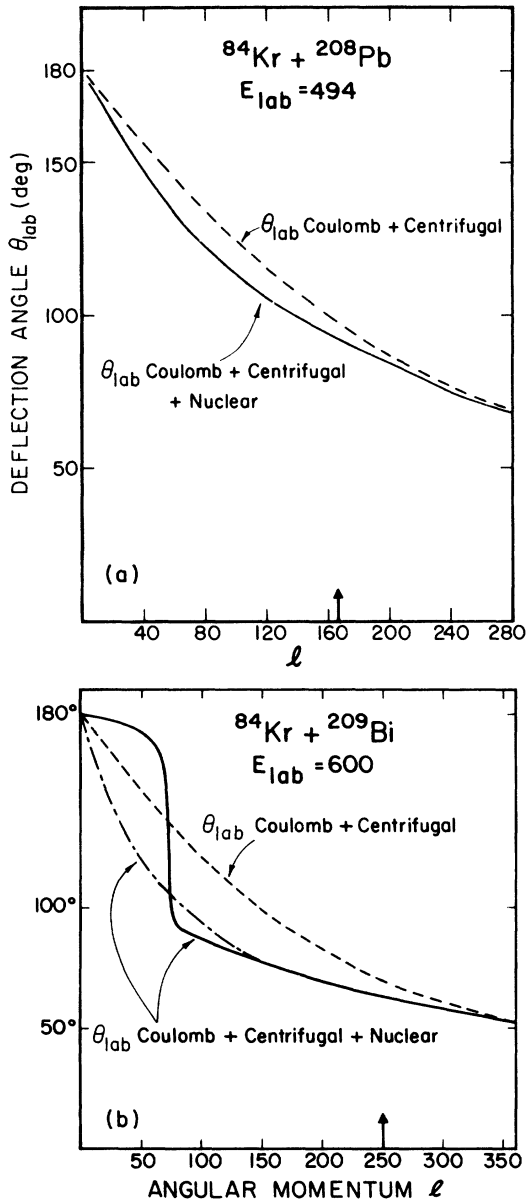

FIG. 6. Deflection functions for (a) 494- and (b) 600-MeV bombarding energy. The nuclear potential was characterized by a Woods-Saxon optical model with $V = 50$ MeV, $R_v = 1.177\,(A_1^{1/3} + A_2^{1/3})$ fm, $a_v = 1.0$ fm, and $W = 2.5$ MeV, $R_w = 1.29\,(A_1^{1/3} + A_2^{1/3})$ fm, and $a_w = 0.38$ fm. At 600 MeV the effect of setting $W = 0.1$ fm is shown by the dot-dashed curve.

absorption, it is not clear which deflection function is most appropriate, but it would appear to us that the model can be expected to give the effect of the imaginary potential property on only the elastic channel. Comparison with coupled-channels calculations might provide a solution to this problem. The present use of the deflection function deduced from the elastic scattering potential has to be considered a first approximation, hopefully giving the lowest order effects of the nuclear potential.

To explore the relation between the deflection function and the angular distribution in more detail we have computed the cross section for deeply inelastic scattering from

$$\left(\frac{d\sigma}{d\Omega}\right)_{\text{deeply inelastic}} = \left(\frac{d\sigma}{d\Omega}\right)_{\text{reaction}} = \left(\frac{d\sigma}{d\Omega}\right)_{\text{cl}} (T_l),$$

where $(d\sigma/d\Omega)_{\text{cl}}$ is the differential cross section for the classical orbit with angular momentum l and where T_l is taken to describe the probability that a particular partial wave is not elastically scattered. Thus, we are assuming that all nonelastic processes lead to deeply inelastic scattering and none to fusion. If some of the lowest partial waves were to lead to fusion, one might want to omit these partial waves in the calculation. For example, if we take the upper limits for the fusion cross section to be 40 mb at 500 MeV and 150 mb at 600 MeV, in a sharp-cutoff approximation the cross section for deeply inelastic scattering would go to zero for angles larger than 150° and 103° at 500 and 600 MeV, respectively. These are larger angles than have been investigated experimentally. The results of a calculation using the formula given above are shown as the solid curves in Fig. 7, where they are compared with the experimental results. The qualitative features of the angular distributions are reproduced although the predicted peak comes at too large an angle. We would like to emphasize at this point that there are no adjustable parameters in these calculations with the deflection function, the cross section being determined solely from the optical potential derived from the fit to the elastic scattering data. Two important effects have, however, been neglected in these calculations. One is inelasticity, which has the effect of leading to larger deflection in the exit channel and a larger deflection angle, contrary to observation. The second is the deformation of the fragments in the exit channel as indicated by the outgoing kinetic energies, which are sub-barrier with respect to the entrance channel. Such fission-like distortions imply that the attractive nuclear potential acts for larger separations in the exit channel than in

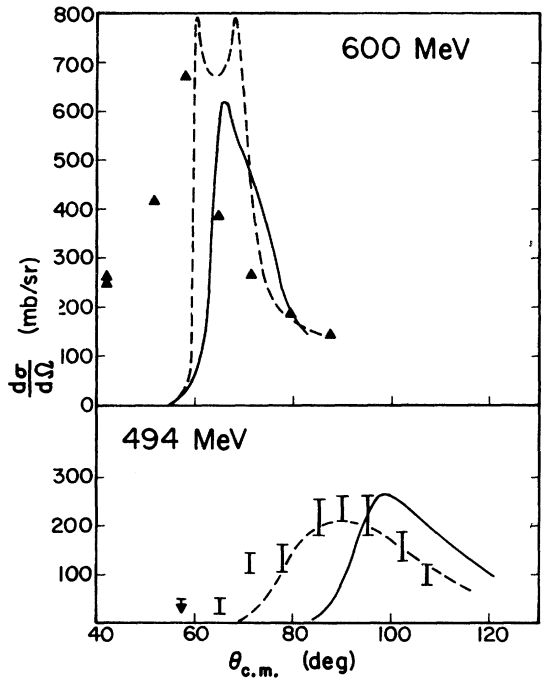

FIG. 7. Comparison of experimental and calculated angular distributions. The 600-MeV data is from Ref. 4. The full curves were calculated using the elastic channel deflection function only. The dashed curves are based on calculations that approximately take into account inelasticity and distortion effects (see text). $d\sigma/d\Omega$ is in units of mb/sr.

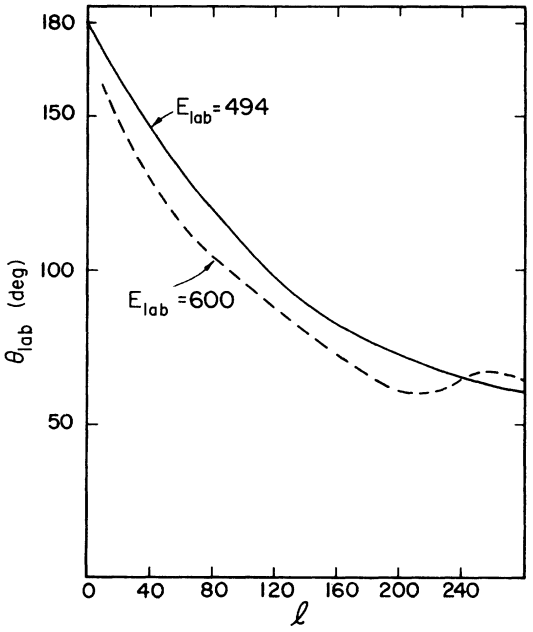

FIG. 8. Deflection functions for (a) 494- and (b) 600-MeV bombarding energy. The effects of distortion in the exit channel and inelasticity are included (see text).

the entrance channel. We have tried to simulate these effects qualitatively by calculating the deflection function for the average exit channel kinetic energy ($E_{c.m.}$ = 275 MeV) with the optical potential scaled to a larger radius to simulate the distortion. An increase of 45% was assumed, in keeping with the estimates of Wolf *et al.*[4] This increase must probably be considered an upper limit. The entrance and exit channel deflection functions were then averaged to obtain the final deflection functions illustrated in Fig. 8. The cross sections obtained with these deflection functions are shown as the dashed curves in Fig. 7. The calculated angular distribution at 600 MeV has two singularities associated with the maximum and minimum on the deflection function; $d\theta/dl$ goes to zero at these points. Such singularities would vanish in a less classical treatment where the spread in angles associated with a particular l is taken into account. Nevertheless, these calculations produce much better agreement with the position of the peak. This success in accounting for the angular distributions solely in terms of the deflection properties and the optical potential suggests to us that it will not be possible to deduce from angular distributions alone quantitative information about nuclear viscosity or friction. The energy spectra should provide better information on these properties.

We have not yet discussed calculations for the 718-MeV data here. At this energy, unlike the lower energies, the deflection is very sensitive to the nuclear potential in the interior region where the potential cannot be unambiguously deduced from elastic scattering. Two potentials obtained in the fitting of the 718-MeV elastic data gave qualitatively different deflection functions for the lower partial waves. There is also a greater sensitivity to the presence of the imaginary potential. We therefore do not feel that the deflection function at high energy is sufficiently well characterized by elastic scattering potentials to be useful in predicting the deeply inelastic scattering.

The dependence of the angle-integrated cross sections for the sum of the deeply inelastic and quasielastic scattering on the bombarding energy has been reported in Ref. 6. It was shown that the observed cross sections are approximately equal to the total absorption cross section calculated from the optical model with parameters that gave a fit to the elastic scattering data.[13] At 500 MeV no direct evidence exists for compound nuclear processes although an upper limit of 40 mb for the fusion process has been estimated.[1] The dominance of deeply inelastic over fusion processes at this bombarding energy is probably not an unexpected result. The Coulomb potential is so strong that even for the lowest partial waves the distance of closest approach for Coulomb trajectories is larger than the sum of the radii characterizing the density distributions of the target and projectile. It is nevertheless possible to have a large cross section even for a reaction that is essentially all a surface reaction. In Fig. 9 we show how a large range of impact parameters are focused into a rather narrow range of distances of closest approach. The abscissa for the lower part of the figure is the impact parameter b; for the upper part it is the distance of closest approach R_{min}. From particular b values along the lower line we have drawn connecting lines so as to indicate the corresponding values of the distance of closest approach on the upper abscissa. We assume Coulomb trajectories in making this correspondence. The inclusion of the nuclear potential employed earlier for the deflection function has little effect on the distance of closest approach at this bombarding energy, decreasing R_{min} by only about 10%. This is because the nuclear potential is weak compared to the Coulomb potential; in fact, for the potential used there is no barrier or minimum in the potential energy curve. The impact parameter values chosen correspond to the values that would give the lower (0) and upper limits to the fusion cross section and the value that would give the observed total nonelastic cross section. The ordinate in Fig. 9 is the differential cross section for a particular distance of closest approach. It

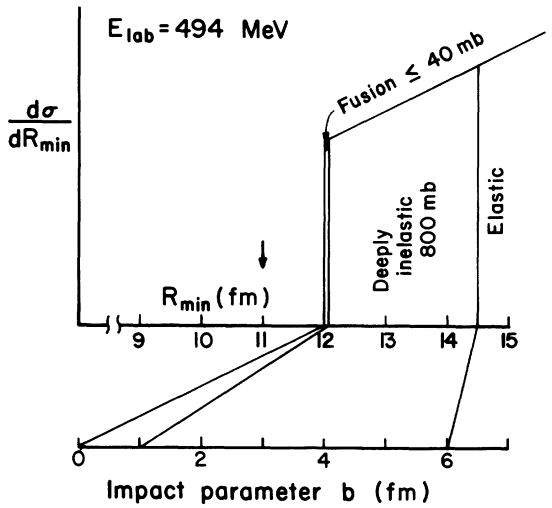

FIG. 9. $d\sigma/dR_{min}$ is shown as a function of R_{min}, the distance of closest approach. Also shown are the corresponding impact parameters for Coulomb trajectories; the solid lines define the range of distance of closest approach associated with a given range of impact parameters. The values chosen correspond to the values that would give the upper and lower limits to the fusion cross section and the value that would give the observed total nonelastic cross section.

can be seen that because of the very strong Coulomb repulsion, a relatively large range of impact parameters (and hence a large cross section) is associated with a narrow range of distances of closest approach. Thus most, if not all, impact parameters can be thought of as leading to surface reactions, with the implied surface region of 2 fm being comparable with that implied by direct reaction cross sections for lighter particles. The arrow pointing toward the abscissa of the upper part of Fig. 9 indicates the separation distance at which the nuclear density reaches its saturation value at the point of contact.

The situation at the higher bombarding energy of 718 MeV is different. Here the Coulomb repulsion is less effective and there is a considerably larger range of distance[6] of closest approach. Galin *et al.*[7] have proposed a criterion as to whether the target and projectile will fuse based on the concept of whether the distance of closest approach is smaller than some critical radius. If one calculates the fusion cross section expected according to this criterion, one expects 1200 ± 200 mb at 718 MeV which is one and one half times larger than the upper limit we have deduced for a possible fusion-fission contribution.[6] Possible reasons for the inhibition against fusion have been discussed previously.[6]

The interaction potential at the radius at which nonelastic reactions set in can be deduced from the energy dependence of the reaction cross section through the classical expression

$$\sigma_R = \pi R^2 \left(1 - \frac{V_{\text{int}}}{E}\right) .$$

(It is not necessary that an actual barrier exist for application of this formula—only the assumption of angular momentum conservation and that absorption sets in at a fairly well defined interaction distance R.) We take the integrated deeply inelastic cross section to equal the reaction cross section. This assumption is supported by the near equality of the integrated deeply inelastic cross section and the optical model absorption cross section. From a plot of σ_R vs $1/E$, V_{int} is found to be 310 ± 22 MeV and the interaction radius $R = 14.3$ fm, in good agreement with the value obtained in the analysis[13] of the elastic scattering. This value of 14.3 fm corresponds to $R = 1.4(A_1^{1/3} + A_2^{1/3})$ consistent with values obtained in other systems with heavy projectiles and targets.[16,17] The Coulomb potential at 14.3 fm is 298 MeV so that the deduced V_{int} is consistent with the small value of the nuclear potential used in the deflection angle calculations. This potential is only a few MeV deep at this distance.

We turn now to a discussion of the exit channel total kinetic energy and its dependence on angle. It has already been noted[1,4] that the most probable total kinetic energy is rather low, more typical of the Coulomb repulsion between spherical partners. It can be seen in Figs. 3 and 4 that the most probable kinetic energy depends on the angle of emission. At the highest bombarding energy there is a considerable recession in energy at angles both smaller and larger than the angle at which the cross section is largest. If the energy loss is dependent on the extent to which the fragments overlap (and "rub against each other"), this recession would suggest that the trajectories corresponding to angles both smaller and larger than the grazing angle might correspond to a greater overlap of the nuclear matter density of the target and projectile. Although the deflection function at 500 MeV does not indicate such an effect, the character of the deflection function at 600 MeV might be consistent with such an interpretation. A possible test of this hypothesis would be to measure the mass or charge transfer as a function of angle. Wolf *et al.*[4] found more mass transfer at an angle backward of the peak angle than at an angle nearer the peak angle. It would be interesting to see if the transfer probability increases again at angles well forward of the peak.

Another very remarkable feature of the present results is that as the entrance channel center of mass energy is increased 150 MeV in going from 494 to 718 MeV, the kinetic energy distribution still extends to energies below that for the Coulomb repulsion of two spherical fragments. As has been noted, however, for the more peripheral collisions the mechanism responsible for damping is not as effective at the higher energies. Nevertheless over 200 MeV of energy can be transferred from kinetic energy to excitation energy in a time so short that the angular distribution remains peaked quite similar to that expected to result from grazing trajectories.

V. SUMMARY

We have reported the bombarding energy dependence of the angular distributions, kinetic energy release, and angle-integrated cross sections for emission of projectile-like reaction products for the reaction of ^{84}Kr with ^{208}Pb. Essentially all of the expected absorption cross section appears as quasielastic or deeply inelastic events, even at bombarding energies where the incident energy is well in excess of the Coulomb barrier. The qualitative features of the angular distributions are consistent with a semiclassical approach where the distortion of the trajectory by Coulomb and nuclear forces is taken into account. Allowing for nuclear distortion of the fragments in the exit channel leads to a better description of the angular distributions

and is consistent with the observation that the exit channel total kinetic energy is often less than that expected for rigid spherical fragments. The energy loss associated with deeply inelastic scattering is found to be angle dependent. Also as the bombarding energy is increased, the energy loss increases, so that the most probable energy for the deeply inelastic peak is approximately independent of the incident energy.

ACKNOWLEDGMENTS

We are grateful to the SuperHILAC staff for their cooperation in providing the beam for these measurements, and to Richard Eppley for assistance in the experimental setup. We thank Michael Zisman for his contributions to the final phases of this work, and Professor Ulrich Mosel for helpful comments.

---

†Research supported in part by the U.S. Energy Research and Development Administration.

[1]F. Hanappe, M. Lefort, C. Ngô, J. Peter, and B. Tamain, Phys. Rev. Lett. 32, 738 (1974).

[2]A. G. Artukh, G. F. Gridnev, V. L. Mikheev, V. V. Volkov, and J. Wilczynski, Nucl. Phys. A215, 91 (1973).

[3]M. Lefort, C. Ngô, J. Peter, and B. Tamain, Nucl. Phys. A216, 166 (1973).

[4]K. L. Wolf, J. P. Unik, J. R. Huizenga, J. Birkelund, H. Freiesleben, and V. E. Viola, Phys. Rev. Lett. 33, 1105 (1974).

[5]J. V. Kratz, A. E. Morris, and G. T. Seaborg, Phys. Rev. Lett. 33, 502 (1974).

[6]R. Vandenbosch, M. P. Webb, and T. D. Thomas, Phys. Rev. Lett. 36, 459 (1976).

[7]J. Galin, D. Guerreau, M. Lefort, and X. Tarrago, Phys. Rev. C 9, 1018 (1974). See also D. Glas and U. Mosel, *ibid.* 10, 2620 (1974).

[8]J. Wilczynski, Phys. Lett. 47B, 45 (1973).

[9]M. P. Webb, R. Vandenbosch, and T. D. Thomas (unpublished).

[10]K. L. Wolf, J. R. Huizenga, J. Birkelund, H. Freiesleben, and V. E. Viola, Bull. Am. Phys. Soc. 21, 31 (1976).

[11]B. Tamain, F. Plasil, C. Ngô, J. Peter, M. Berlanger, and F. Hanappe, Phys. Rev. Lett. 36, 18 (1976).

[12]K. W. Ford and J. A. Wheeler, Ann. Phys. (N.Y.) 1, 259 (1959).

[13]R. Vandenbosch, M. P. Webb, T. D. Thomas, S. Yates, and A. Friedman, Phys. Rev. C 13, 1893 (1976).

[14]H. L. Harney, P. Braun-Munzinger, and C. K. Gelbke, Z. Phys. 269, 339 (1974).

[15]C. K. Gelbke, Z. Phys. 271, 399 (1974).

[16]A. Fleury and J. M. Alexander, Annu. Rev. Nucl. Sci. 24, 279 (1974).

[17]H. H. Gutbrod, W. G. Winn, and M. Blann, Nucl. Phys. A213, 267 (1973).